Task-based optimization of 3D breast x-ray imaging using mathematical observers

Zhijin LI 06 Oct 2017

Thesis advisors

Agnès Desolneux	CNRS, CMLA - ENS Paris Saclay
Ann-Katherine Carton	GE Healthcare France

X-ray breast imaging

Key x-ray imaging modalities for breast cancer detection & diagnosis

2D FFDM

TOWARDS

3D DBT

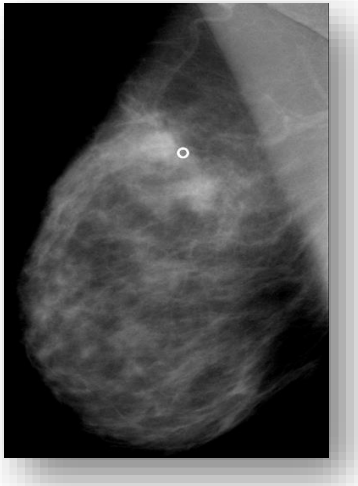

Mammogram

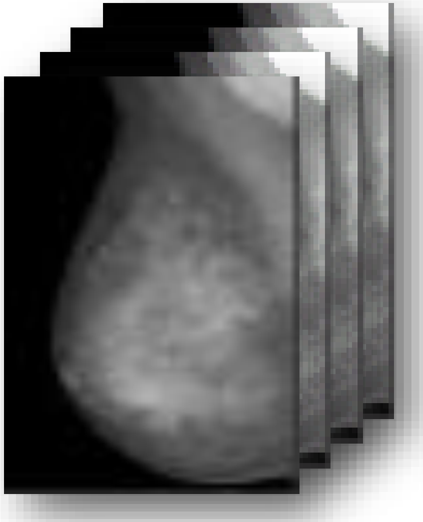

Slices

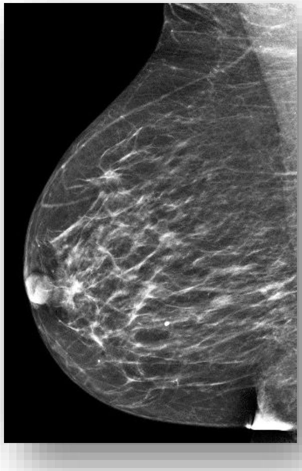

Synthetic 2D mammogram (S2D)

Thesis → focus on 3D
Clinical performance assessment of 3D DBT vs 2D FFDM

Virtual clinical trials (VCT)

Clinical Trials

PATIENT

IMAGING SYSTEM

RADIOLOGIST

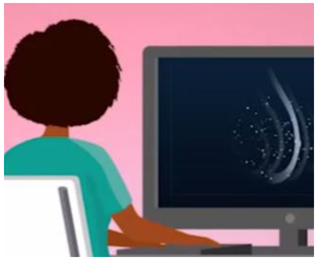

CLINICAL PROTOCOL

Virtual Clinical Trials (VCT)

DIGITAL BREAST

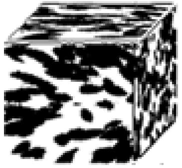

DIGITAL IMAGING SYSTEM

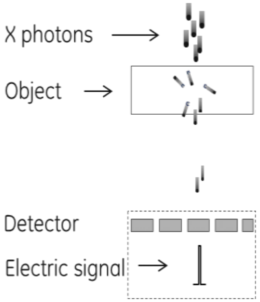

MODEL OBSERVER

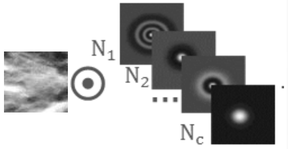

VIRTUAL CLINICAL PROTOCOL

FASTER

- Image acquisition
- Image review
- Ground truth

COST SAVING

- No patient recruitment
- No radiologists involved
- No patient monitoring
- No legal contracts

MORE ACCURATE

- Full knowledge of breast model & pathology

Thesis objectives

µcalc detection performance assessment in 3D DBT vs 2D FFDM & S2D using VCT

Development & validation of VCT tools

- A new 3D mathematical breast texture model
- A new 3D *a contrario* observer for µcalc detection

Models for x-ray breast image simulation

State-of-the-art approaches

3D mathematical random field breast texture models

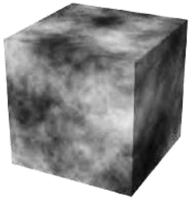

- Power-law Gaussian random field

$$S(f)(\nu) \propto {}^{1}/_{|\nu|^{\beta}}$$

- Clustered lumpy background (shot-noise random field)

$$f(x) = \textstyle\sum_i g(x - y_i; m_i)$$

Anthropomorphic breast phantoms

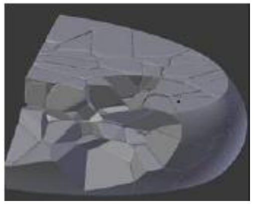

- Model-based

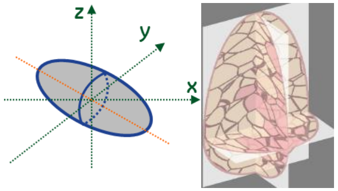

- Empirical data-based

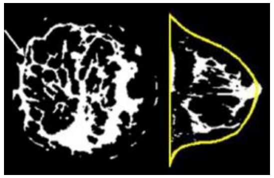

- Hybrid

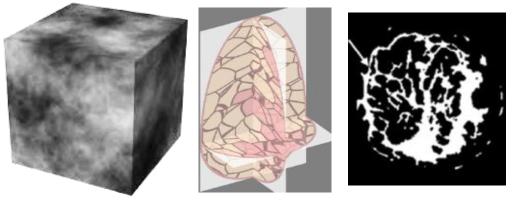

3D Random field breast textures

Volume slice

Projection

3D power-law Gaussian random field

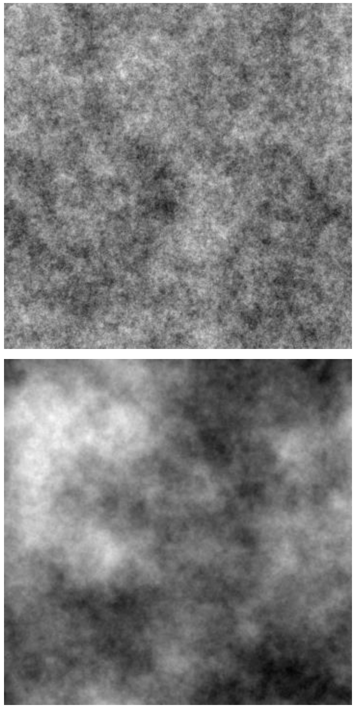

3.5 x 3.5 cm^2

3D clustered lumpy background

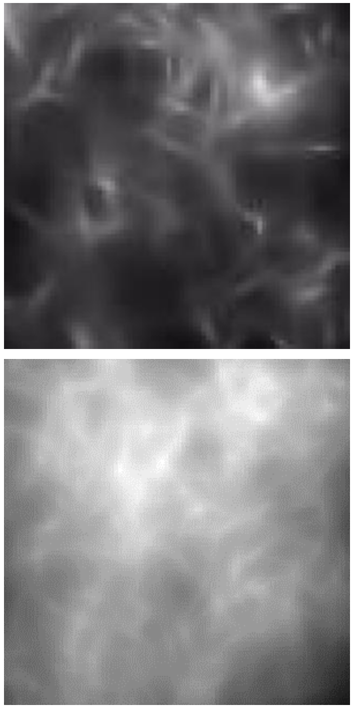

Clinical images

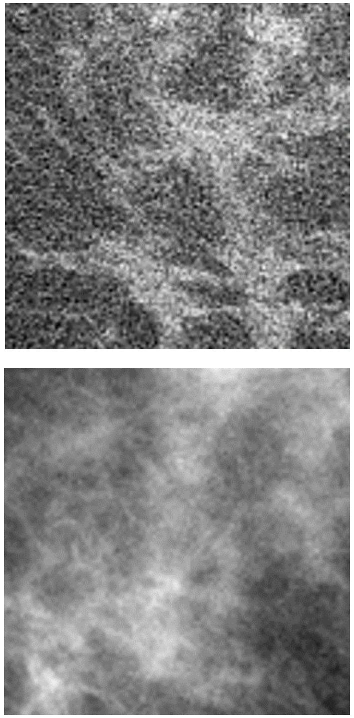

Characteristics

☺ Mathematical traceability

😐 Some statistics match clinical images

☹ Visual realism

☹ Morphological variability vs clinical images

Antropomorphic breast phantoms

Model-based

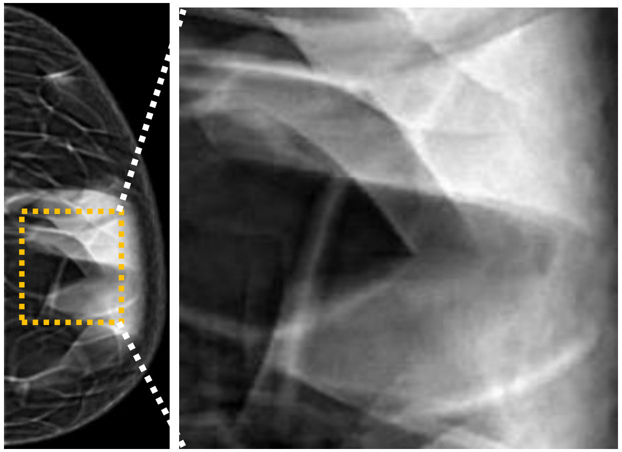

Bakic *et al. (2012)*

Empirical data-based

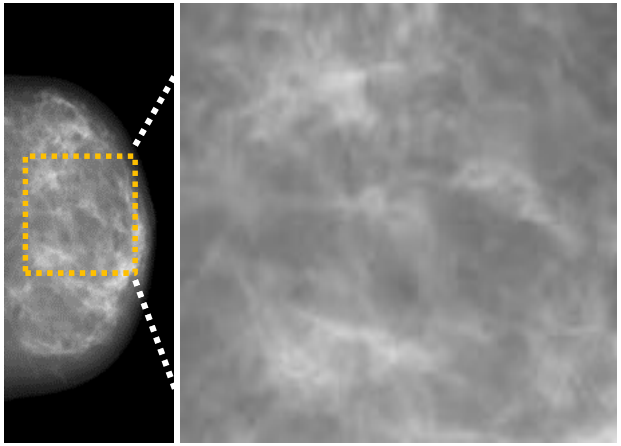

Li et al. *(2013)*

Hybrid

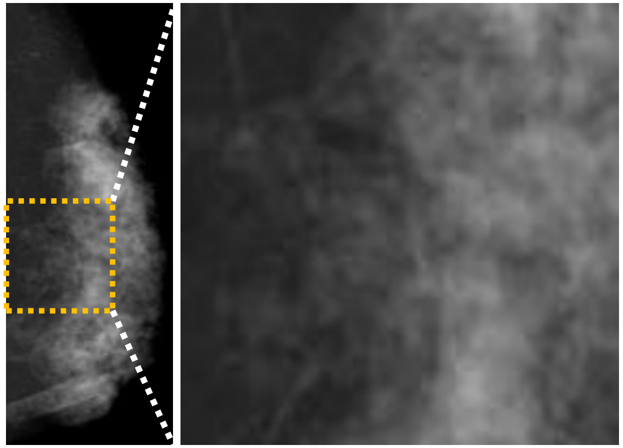

Beverly A. et al. (2012)

Characteristics

😐 – 😊 Visual realism

😐 Morphological variability vs clinical images

☹ Mathematical traceability

GOAL

Develop a new 3D breast texture model that shares the advantages of random field textures & anthropomorphic breast phantoms

Input: clinical breast CT data

Re-projection of segmented breast CT (bCT) data

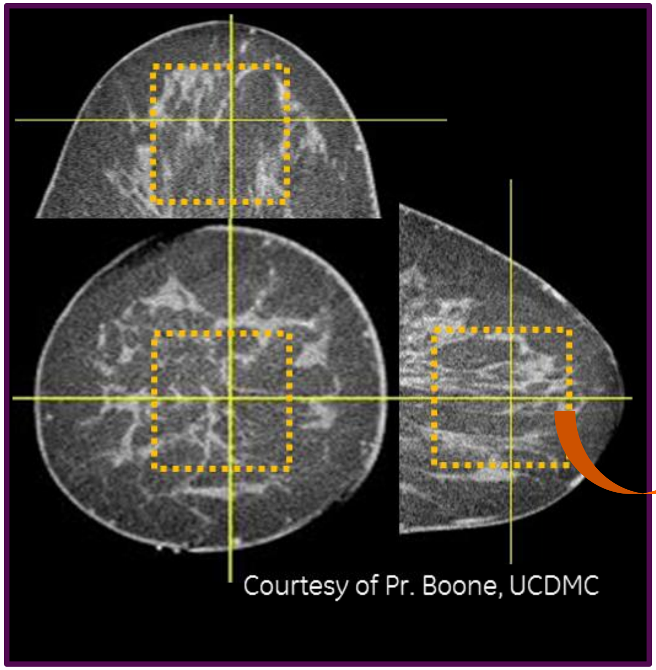
Courtesy of Pr. Boone, UCDMC

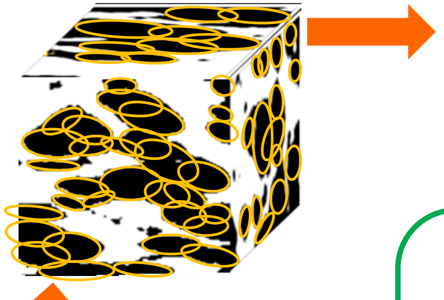

$5 \times 5 \times 5 cm^3$

Extraction & Segmentation

DBT projection simulation

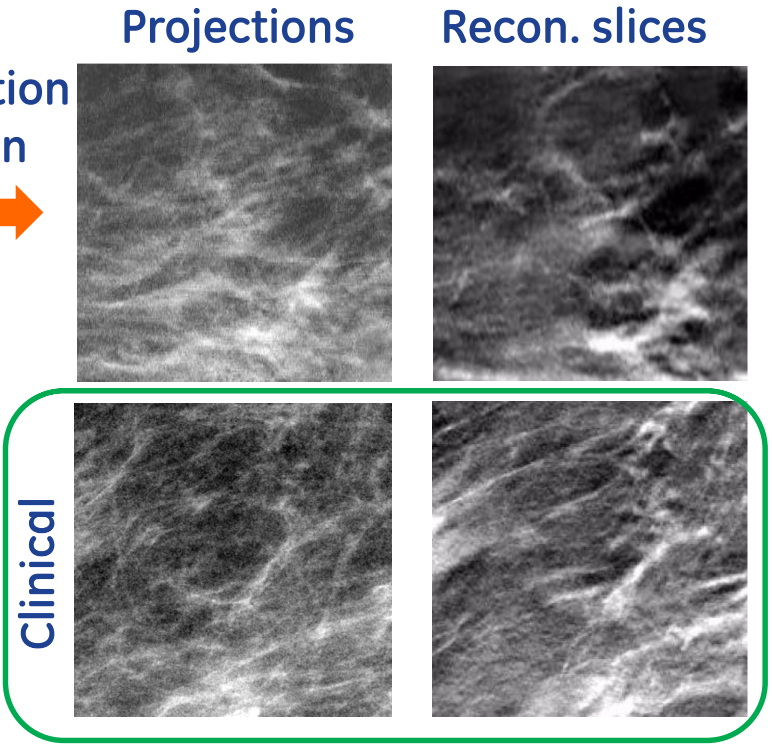

Idea: model tissue morphology & distribution as in bCT

<u>Medium scale</u>

Intra-glandular adipose compartments → Random ellipsoids

<u>Small scale</u>

Adipose compartments boundary irregularity → Voronoi diagram

3D breast texture sampling algorithm

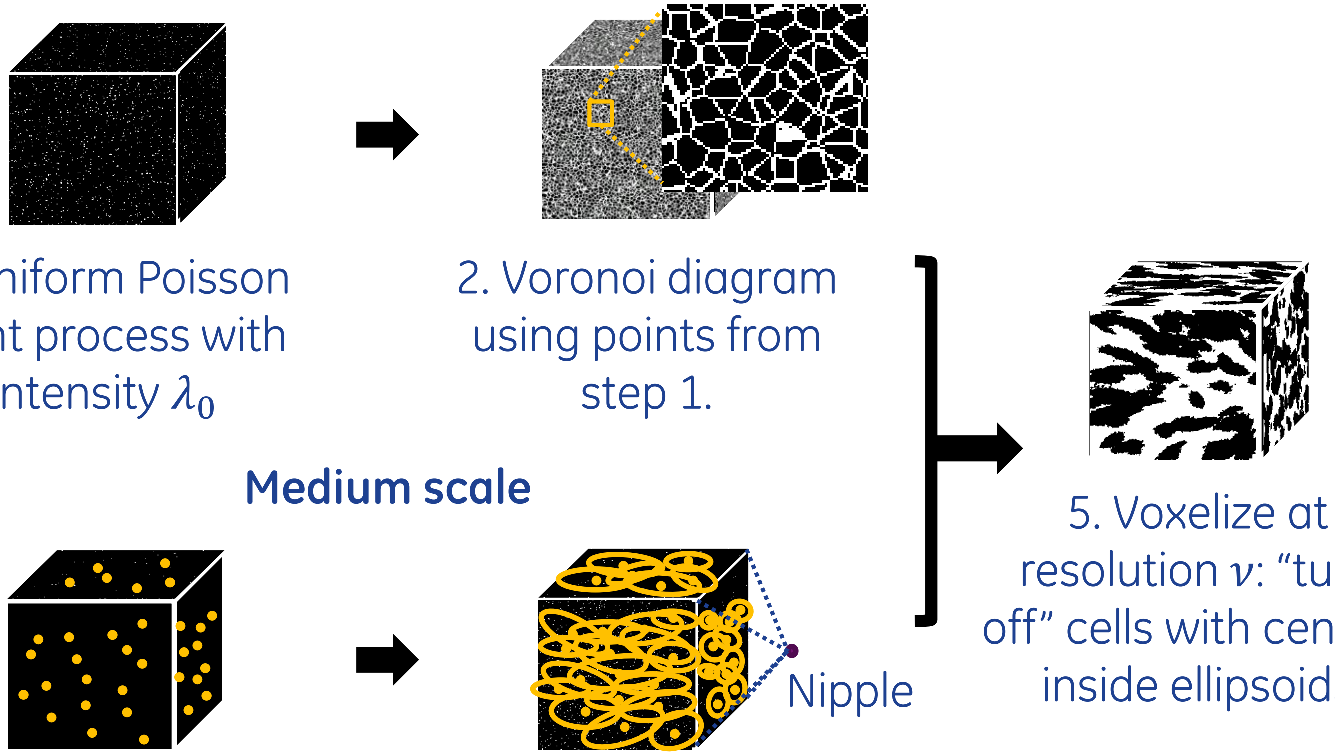

Small scale

1. Uniform Poisson point process with intensity λ_0

2. Voronoi diagram using points from step 1.

Medium scale

3. Seed point process ~ distribution $\mathbf{P}_s$

4. Random ellipsoid ~ distribution $\mathbf{P}_{\boldsymbol{\theta}}$

5. Voxelize at resolution ν: “turn off” cells with centers inside ellipsoids

Simulation results

- Empirically determined parameters
- Simulated using a calibrated virtual x-ray imaging simulator (no compression)

Simulation results

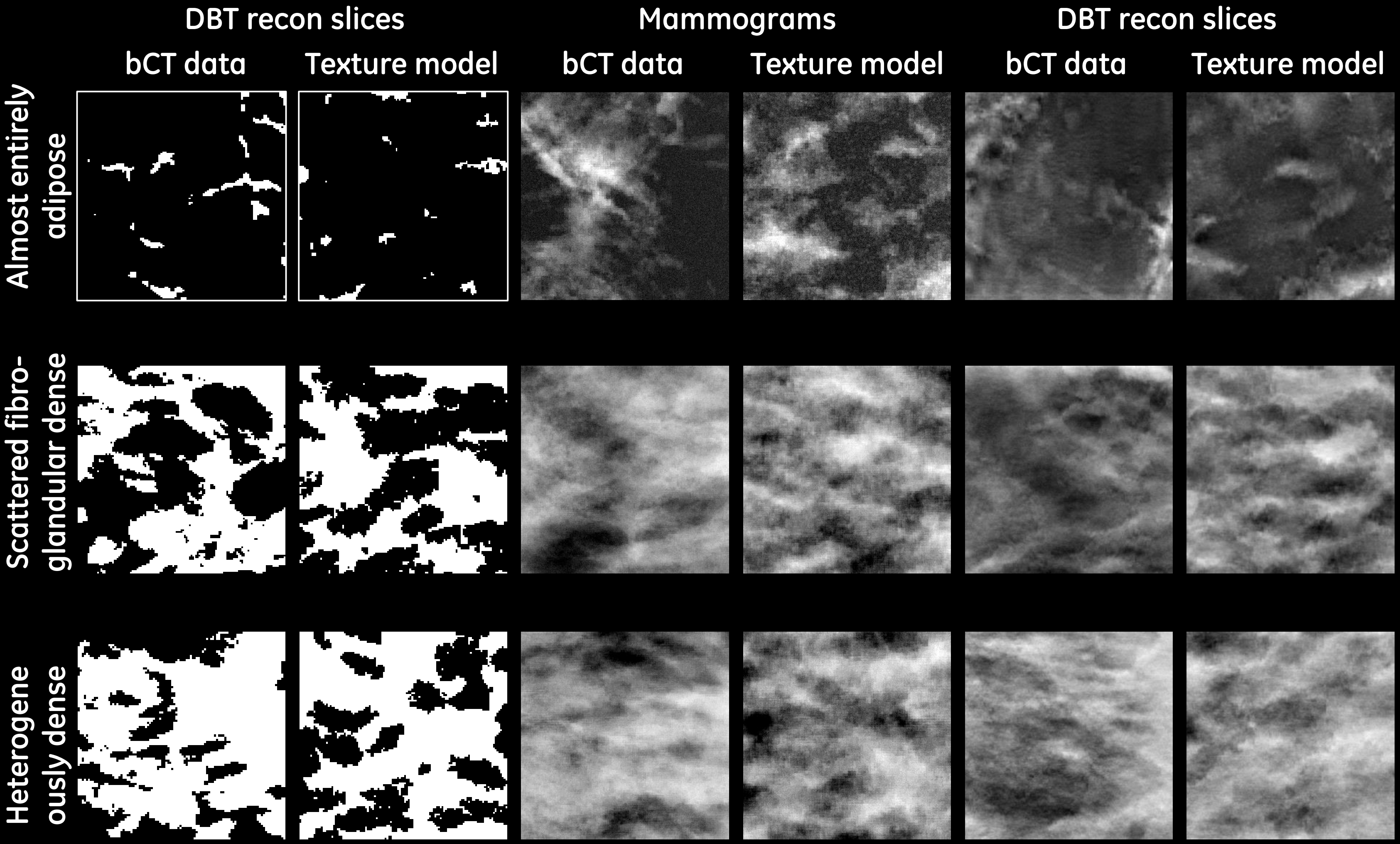

ROI size: 3.5 cm x 3.5 cm

Simulation results: micro-textures

Without Voronoi cells (similar to Mahr *et al*.**)**

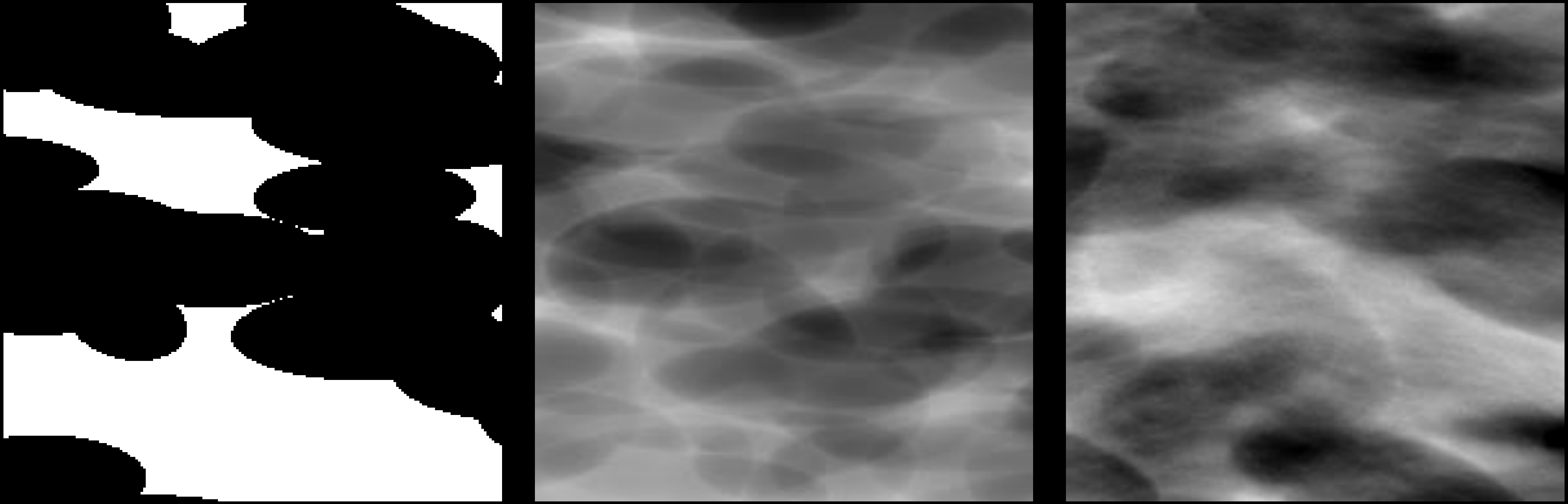

Slice in binary volume **DBT projections** **DBT recon slices**

ROI size: 2 cm x 2 cm

Simulation results: micro-textures

With Voronoi cells (our model)

Slice in binary volume

DBT projections

DBT recon slices

ROI size: 2 cm x 2 cm

Psycho-visual validation of model realism

Two-alternative forced choice experiment

- Darkened room
- ≈ 40cm observer-to-image distance
- Display with 100% images resolution

Clinical bCT bCT **OR** texture model

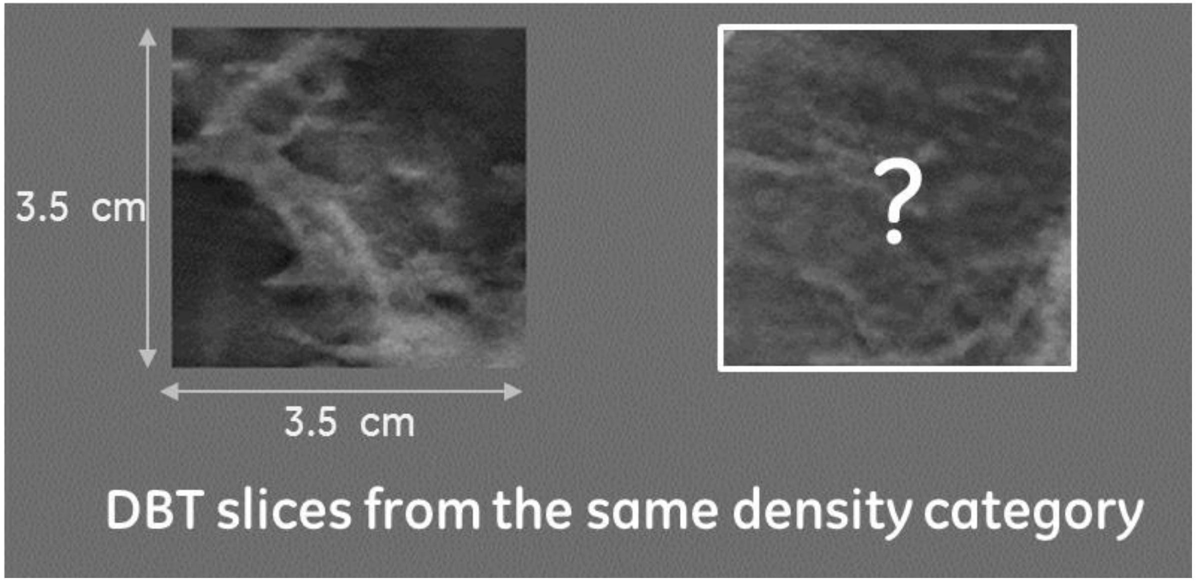

Task

Image on the right: from clinical bCT?

→ Yes OR No

Psychophysical validation of model realism

Experimental result

- Percentage of correct answers (0.5 = observer random guess)

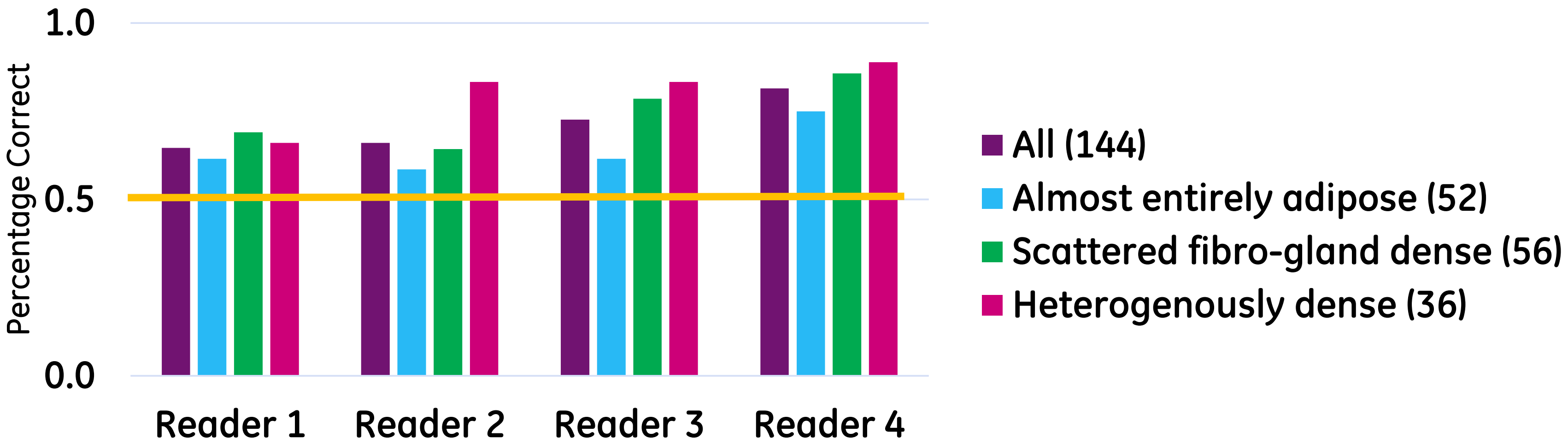

- Almost entirely adipose breast images
  - ✓ Fairly realistic
- « Block artifacts » mostly in dense images

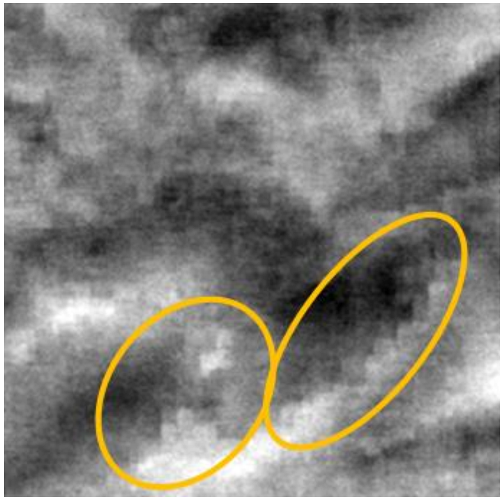

Statistical inference of model parameters

GOAL

Objectively infer medium scale model parameters from segmented clinical bCT volumes of interest

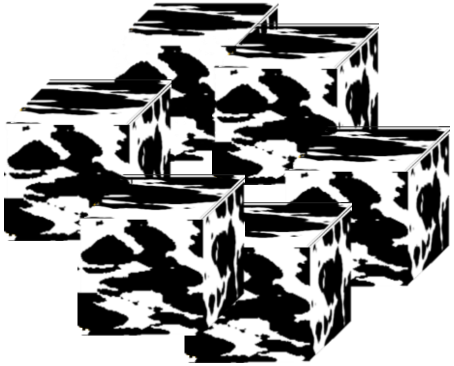

Clinical segmented bCT volumes of interests (VOIs) w/ diff. density

Statistical inference

Medium scale parameters

- Seed point process

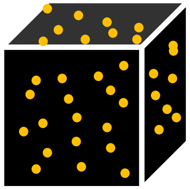

- Ellipsoid parameters

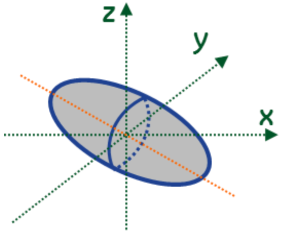

Problem statement

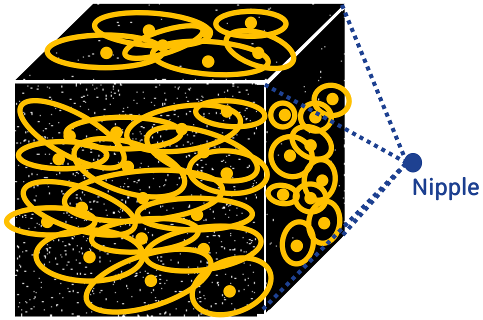

Medium scale model as a marked point process (MPP)

$$Y = \{\boldsymbol{\Phi}_{\boldsymbol{s}}, \boldsymbol{\theta}\}$$

- $\boldsymbol{\Phi}_{\boldsymbol{s}}$: ellipsoid centers point process $\sim \mathbf{P}_{\boldsymbol{s}}$.
- $\boldsymbol{\theta}$: ellipsoid parameters (marks) $\sim \mathbf{P}_{\boldsymbol{\theta}}$.

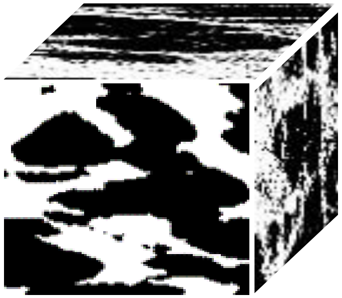

Input bCT VOIs: binary volume

$$D(x) = \begin{cases} 1, \text{if x} \in \text{fibroglandular} \\ 0, \qquad\quad \text{if x} \in \text{adipose} \end{cases}$$

✓**Focus on medium scale: 3.5 x 3.5 x 3.5 cm^3**

Inference is ill-posed

☹ Ellipsoid centers NOT observable

OR

?

Classical MPP parameter inference approach

Minimum contrast estimator

$$\hat{\boldsymbol{\Theta}} = \mathrm{argmin}_{\boldsymbol{\Theta}} \mathcal{C}(\mathcal{D}, \boldsymbol{\Theta})$$

$\boldsymbol{\Theta}$: joint model parameter vector
C: contrast function

Often

$$\mathcal{C}(\mathcal{D}, \boldsymbol{\Theta}) = \iint_{Y \times Y} \Big(\underset{\downarrow}{S}(y_1, y_2; \boldsymbol{\Theta}) - \underset{\downarrow}{\hat{S}}(y_1, y_2; \mathcal{D}) \Big)^2 \mathrm{d}y_1 \mathrm{d}y_2$$

- **Analytical 2nd order statistics** (f.e. pair-correlation function)

- **Empirically measured conter-part of S**

Challenges

- S necessitates a priori model
- Analytical derivation of S: difficult when MPP is complex

Inference from reconstruction

Two-step approach

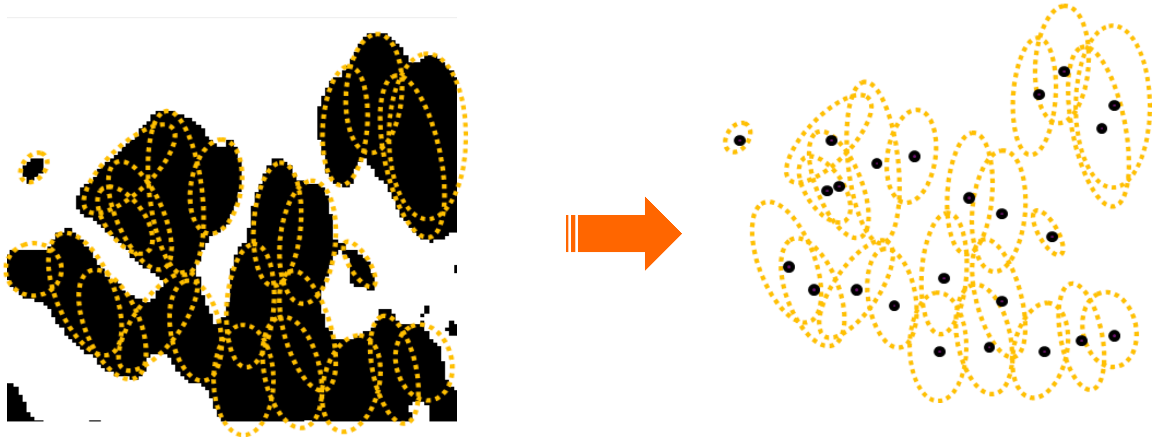

1.Reconstruction step: simulate ellipsoidal approximation

2.Inference step: using reconstructed ellipsoids

Advantages

- Ellipsoid centers observable after reconstruction → facilitate inference
- Reconstruted ellipsoid → intuitions to determine model type

The reconstruction step

GOAL: find an optimal ellipsoidal approximation of input data

Hypothesis

Y: a marked point process with Gibbs density

$$f_{\mathbf{Y}}(\mathbf{u}) = \frac{1}{Z}\exp\left(-\frac{1}{T}U(\mathbf{u})\right)$$

With energy $U(\mathbf{u}) = \mathcal{L}(\mathbf{u},\mathcal{D}) + \mathcal{P}(\mathbf{u})$

The data term

- How a configuration of ellipsoids deviates from input data

The prior term

- Constraint on the overlap percentage btw ellipsoids

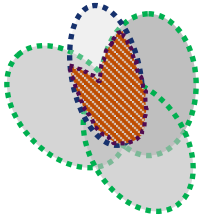

The optimal ellipsoidal configuration u*

$$\mathbf{u}^* = \arg\min_{\mathbf{u}} \left(\mathcal{L}(\mathbf{u},\mathcal{D}) + \mathcal{P}(\mathbf{u})\right)$$

Multiple births, deaths & shifts

- **Initialization**: $n = 1, \boldsymbol{u}^0$, intensity ν^0, ellipsoidal distribution f_θ, temperature T^0, $\delta \in (0, 1)$.
- **Iteration:** at interation n
  - **Multiple births**:

    Generate ellipsoids $\boldsymbol{u}_b \sim (\nu^n, f_\theta)$

    $$\boldsymbol{u}^n = \boldsymbol{u}^{n-1} \cup \boldsymbol{u}_b.$$
  - **Deaths / Shifts**

    For each ellipsoid $u_i \in \boldsymbol{u}^n$, compute *

    $$r = \frac{\alpha \nu^n}{1 + \alpha \nu^n}$$

    Where

    $$\alpha = \exp\left(\frac{U(\boldsymbol{u}^n) - U(\boldsymbol{u}^n \backslash u_i)}{T^{n-1}}\right)$$

    Draw $p \sim \mathrm{Unif}(0,1)$.

    if $p < r$
      - **Death:** remove ellipsoid u_i

    else:
      - **Shift:** u_i→ $\mathcal{L}(u_i)$
  - **Update:**

    $$n \rightarrow n + 1, T^{n+1}, \nu^{n+1} \rightarrow \delta T^n, \delta \nu^n$$
- **Convergence**: energy variation in 10 consecutive runs < ϵ

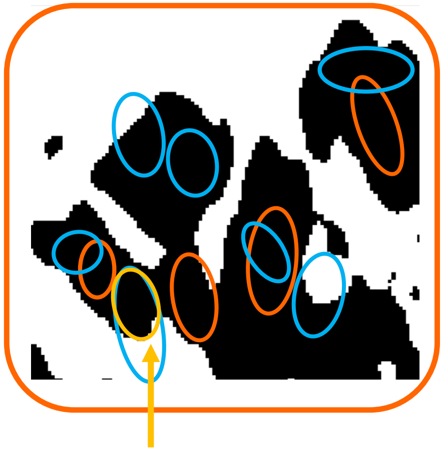

$\mathcal{L}(u_i)$: Legendre ellipsoid: The optimal ellipsoid for the covered adipose region

* **X. Descombes.** Stochastic geometry for image analysis.

Reconstruction result

- Focus on medium scale: not small scale
- Projection: sum of the volume in one direction
  → no x-ray noise

Reconstruction result

Image size: 3.5 cm x 3.5 cm

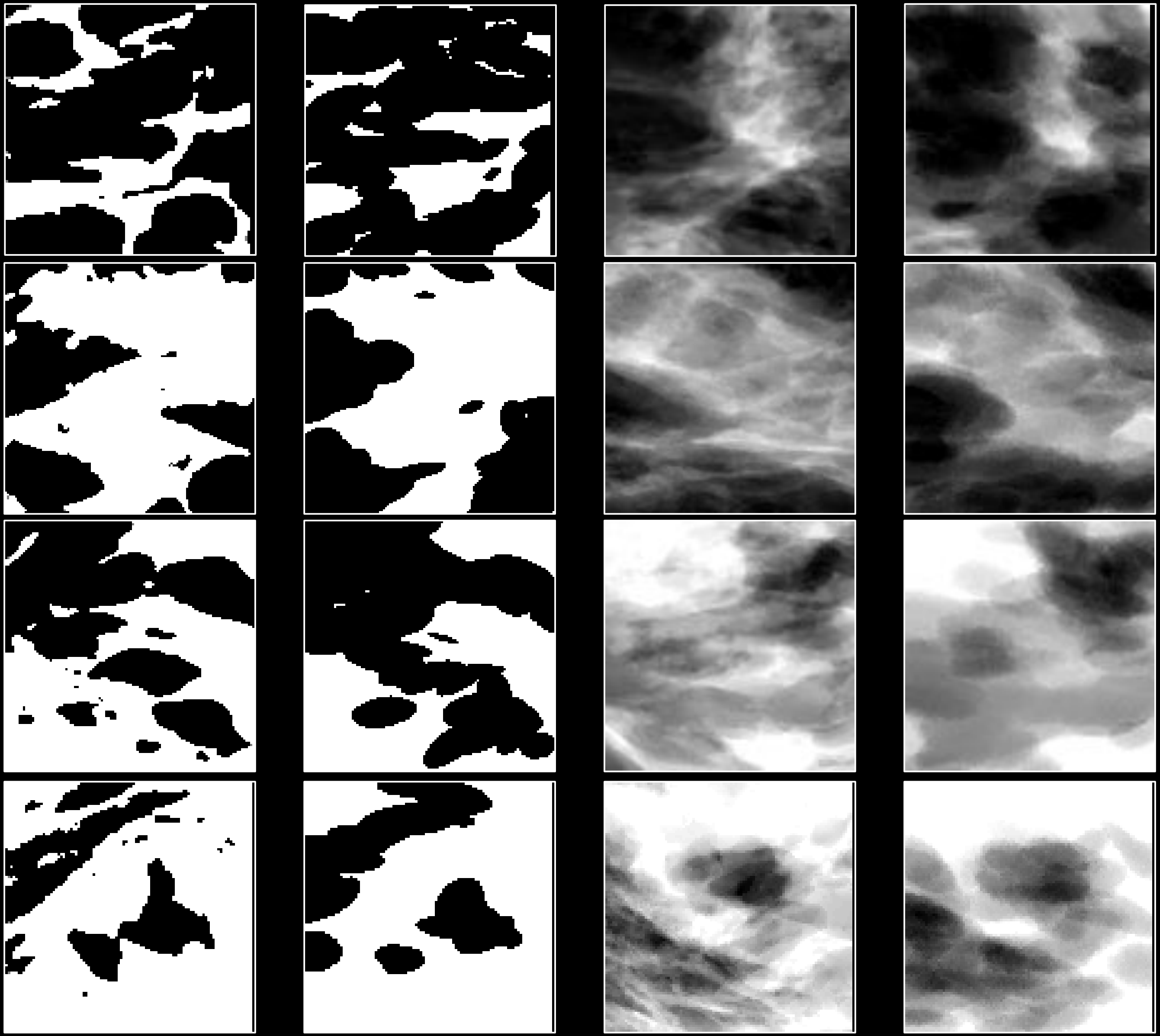

The inference step

GOAL: recon. ellipsoids → center point process, axis lengths & orientation

Reconstructed ellipsoids centers

- Analysis of pair-correlation function (PCF)

$$\mathrm{PCF}(x,y) = \frac{\rho^{(2)}(x,y)}{\lambda(x)\lambda(y)} \quad \text{with} \quad \int_{B_1\times B_2} \rho^{(2)}(x,y)\,\mathrm{d}x\mathrm{d}y = \sum_{x,y\in\Phi}^{x\neq y} \mathbb{E}\left(\mathbb{1}(\{x,y\}\in B_1\times B_2)\right)$$

- Stationary & isotropic process: $\mathrm{PCF}(x,y) = \mathrm{PCF}(r), r = \|x-y\|$

Poisson

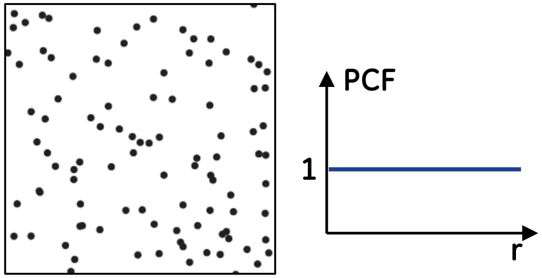

Matérn cluster
$\boldsymbol{\Phi_{\mathcal{M}}(R,\lambda_P,\lambda_C)}$

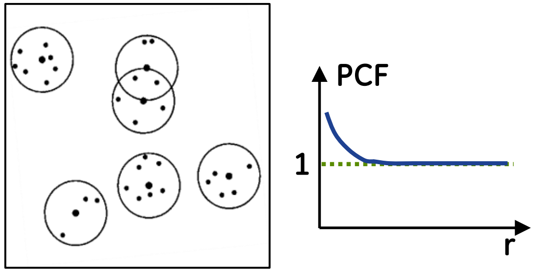

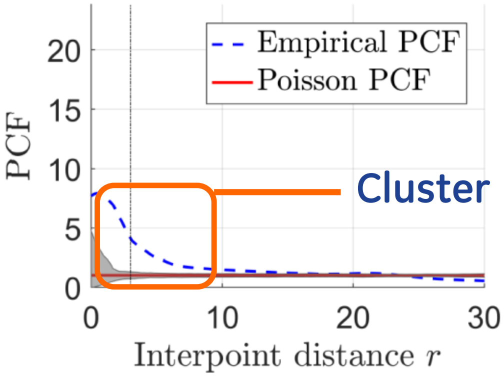

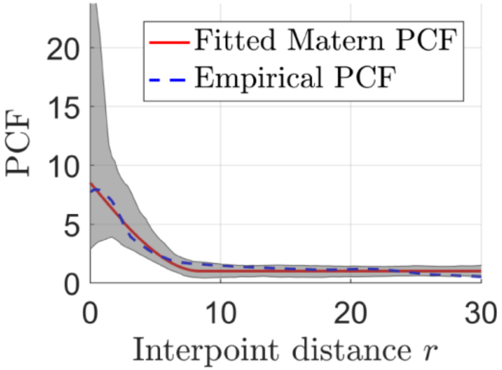

Fit a Matern cluster point process $\boldsymbol{\Phi_{\mathcal{M}}(R,\lambda_P,\lambda_C)}$ using minimum contrast estimator.

The inference step

GOAL: recon. ellipsoids → center point process, axis lengths & orientation

Reconstructed ellipsoids axis lengths & orientation angles

- Analysis of empirical histograms

Axis lengths

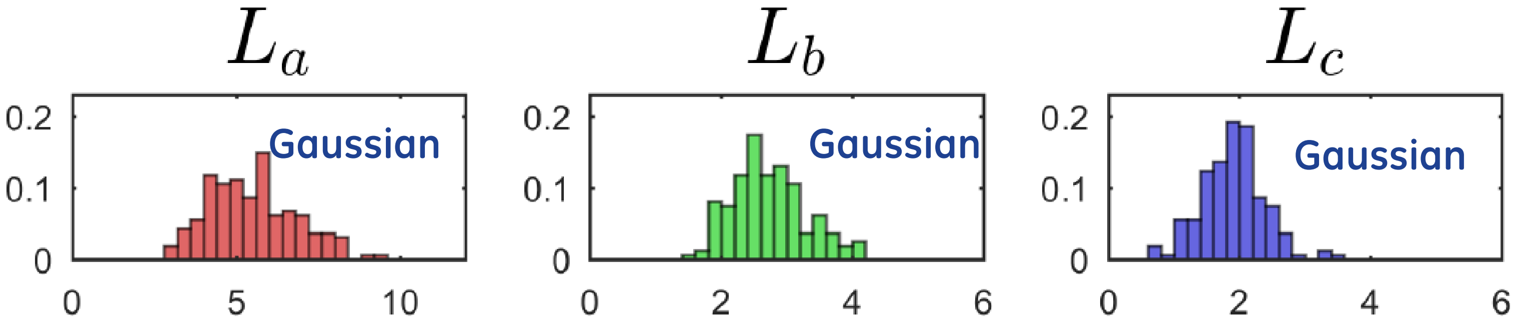

Orientation angles

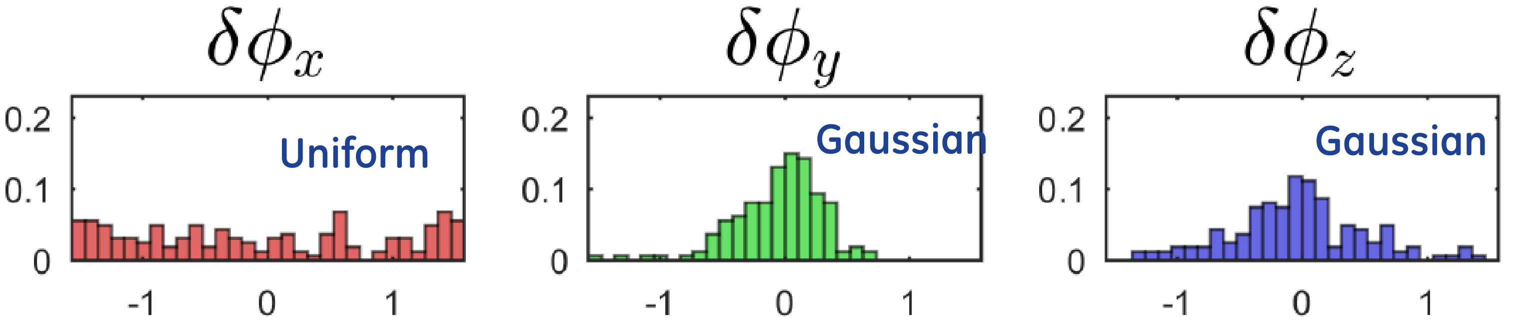

Fitted to Gaussian / Uniform distributions using maximum likelihood estimator

Simulation results using inferred parameters

- Small scale parameter as in the empirical model
- Simulated using a calibrated virtual x-ray imaging simulator (no compression)

Simulation results using inferred parameters

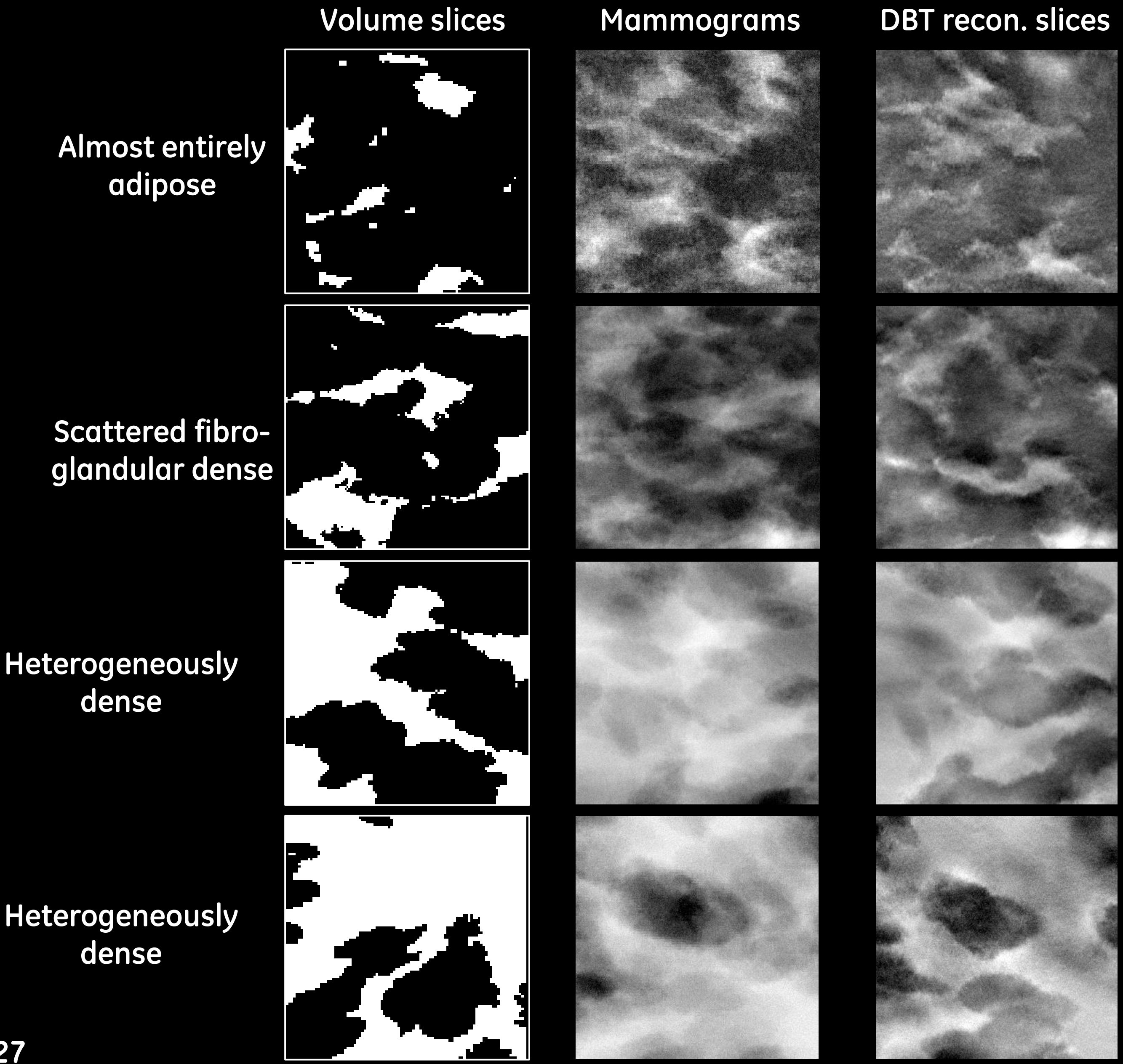

Image size:
3.5 cm x 3.5 cm

Model observer for lesion detection task

Image g → Decision variable $\lambda = f($ images, template, internal noise $)$ → Threshold → Decision outcome D → Figure-of-merit

- **Decision function f**

  → Decision variable λ: observer's confidence of lesion presence.

- Linear observer

$$\lambda = \mathbf{w}^T \mathbf{g}$$

$\mathbf{w}$: template

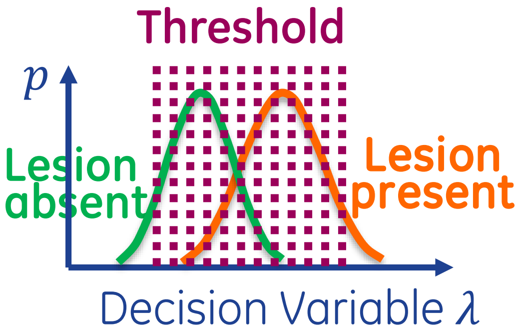

Area under the ROC curve (AUC)

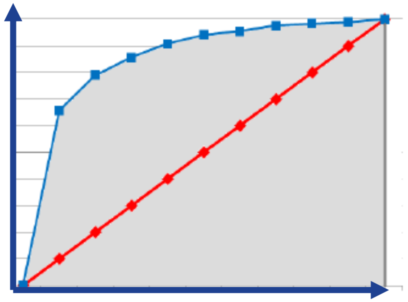

Channelized Hotelling observer

CHO: one of the state-of-the-art for linear model observers

- Based on linear discriminant analysis
- Extendible to 3D volumetric & multi-slice cases

Training phase: compute template $\mathbf{w}_{\mathrm{CHO}}$

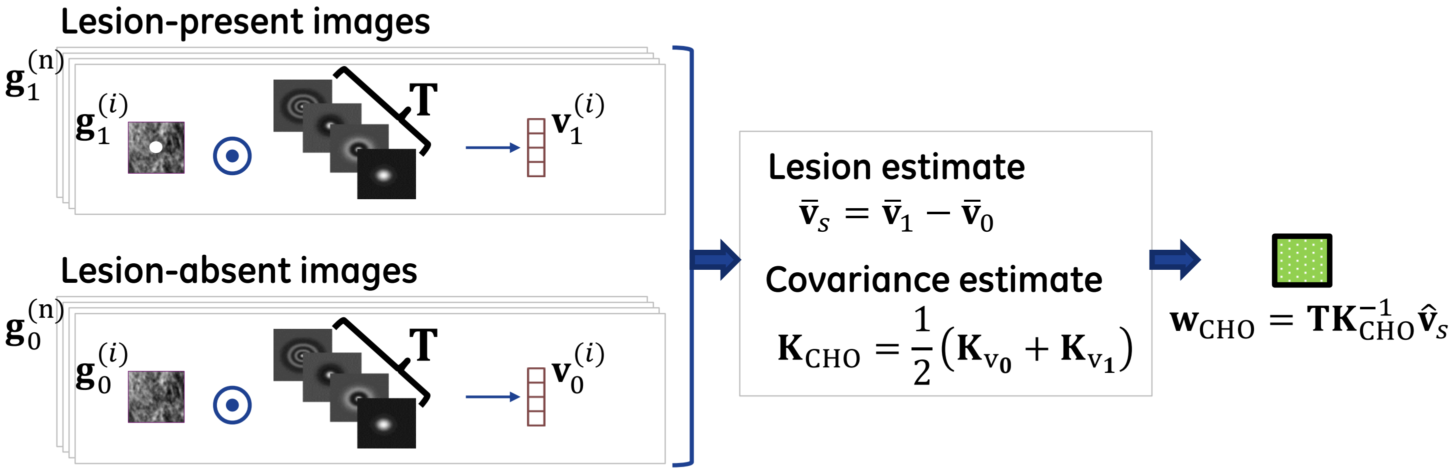

Lesion estimate

$$\bar{\mathbf{v}}_s = \bar{\mathbf{v}}_1 - \bar{\mathbf{v}}_0$$

Covariance estimate

$$\mathbf{K}_{\mathrm{CHO}} = \frac{1}{2}\left(\mathbf{K}_{\mathbf{v}_0} + \mathbf{K}_{\mathbf{v}_1}\right)$$

$$\mathbf{w}_{\mathrm{CHO}} = \mathbf{T}\mathbf{K}_{\mathrm{CHO}}^{-1}\hat{\mathbf{v}}_s$$

Test phase: compute decision variable $\boldsymbol{\lambda}$

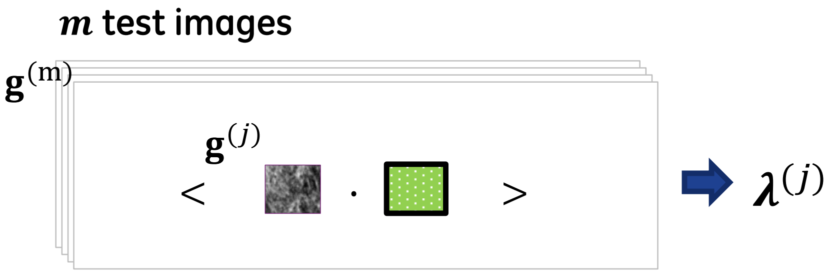

- Myers *et al*. “Addition of a channel mechanism to the ideal observer model”. JOSA (1987)
- Platiša, L. *et al*. “Channelized Hotelling observers for the assessment of volumetric imaging data sets”. JOSA. (2009)

A contrario observer

Principles of *a contrario* detection *

- Based on statistical test
- Quantify the significance of an observed / measured event in a statistically random image.

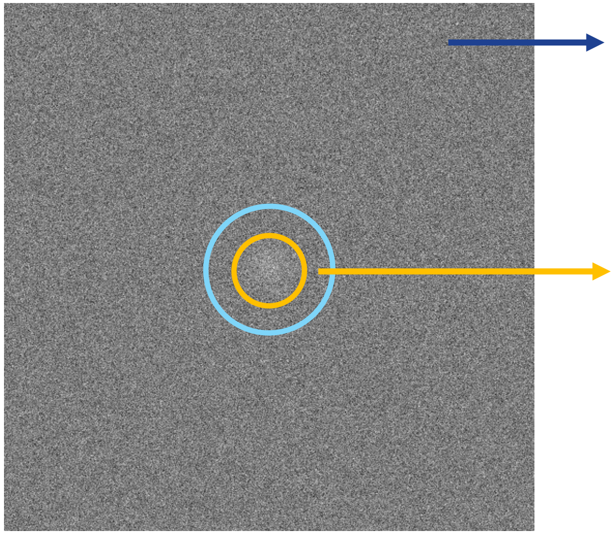

Detection of spot in white noise image*

Naive model

- The null-hypothesis H_0: noise / background model

Measurements $\{M_i\}_i$

- Local characteristics related to the event of interest
- F.e. local contrast

Number of false alarms (NFA) $\{NFA_i\}_i$

- Quantifies how a measurement deviates from the naive model

Thresholding on NFA

- Global false positive control

$$E(|\{NFA_i < \varepsilon\}_i| \mid H_0) < \varepsilon$$

- Desolneux, A., Moisan, L., and Morel, J.-M. From gestalt theory to image analysis: a probabilistic approach. Springer Science & Business Media
- Grosjean, B. and Moisan, L. "A-contrario Detectability of Spots in Textured Backgrounds". Journal of Mathematical Imaging and Vision

Motivations & goals

A new *a contrario* observer

- **Focus on µcalc detection performance in 3D x-ray breast imaging**
  - 2D FFDM vs 3D DBT: results from clinical studies → non-consistent
  - µcal detection performance in S2D vs FFDM: limited research done

- Grosjean, B. "Lesion Detectability in Digital Mammography: Impact of Texture".

Design of a new *a contrario* model observer

1. For pixel x: local naive model

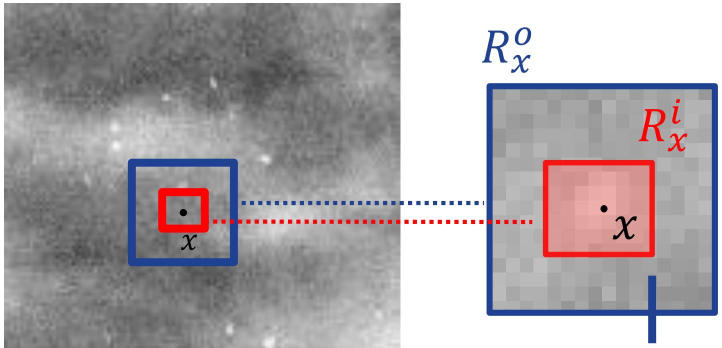

Neighborhood V_x: less than 5 x 5 mm^2

→ Local detection characteristic*

- 🟥Inner rectangle R_x^i: excluded.
  → Exclude possible µcal
- ☐Outer rectangle R_x^o.

Local naive model

- White Gaussian noise
- μ, σ: empirically estimated from neighborhood

- Bochud *et al*. "Estimation of the noisy component of anatomical backgrounds". Medical physics (1999)
- Zhang *et al*. "Adaptive detection mechanisms in globally statistically nonstationary-oriented noise". JOSA (2006)

Design of a new *a contrario* model observer

2. For pixel x: multi-scale NFA

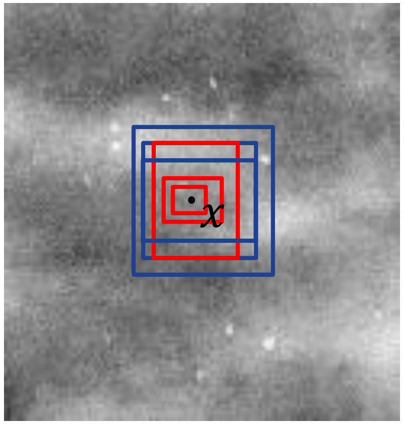

To consider multiple ucalc size & extent

- Multiple-scale neighborhood
- Each scale
  - → Measurement: $g(x)$
  - → compute the NFA

NFA = $N_T\ \Phi(\frac{g(x)-\mu}{\sigma})$

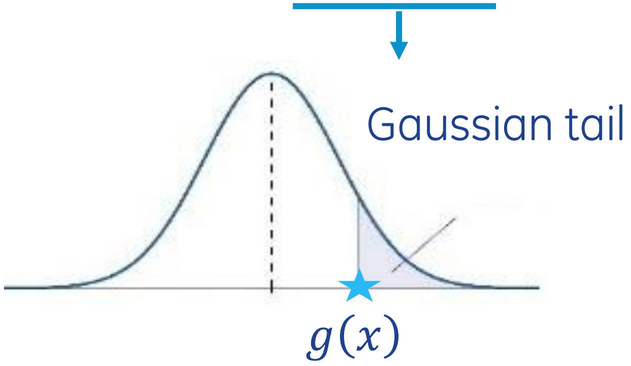

Design of a new *a contrario* model observer

3. For the whole image: decision variable image λ

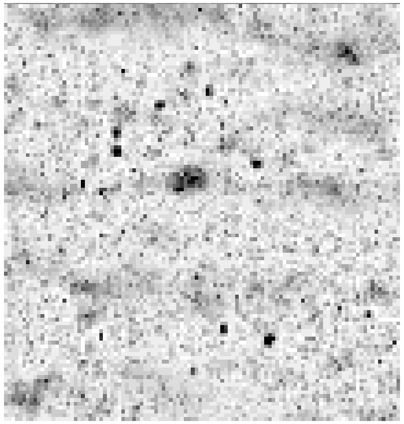

Scan through all pixels

- Take min NFA of all scales for each pixel

$$\boldsymbol{\lambda}(\mathbf{x}) = N_T \ \min_{c \in C} \Phi\left(\frac{g(x)-\mu_c}{\sigma_c}\right)$$

Extension to location known exactly detection in 3D DBT slices

- Size of µcalcs (typically < 1mm) < distance btw two DBT slices (1mm)
- Adjacent DBT slices: weak spatial correlation

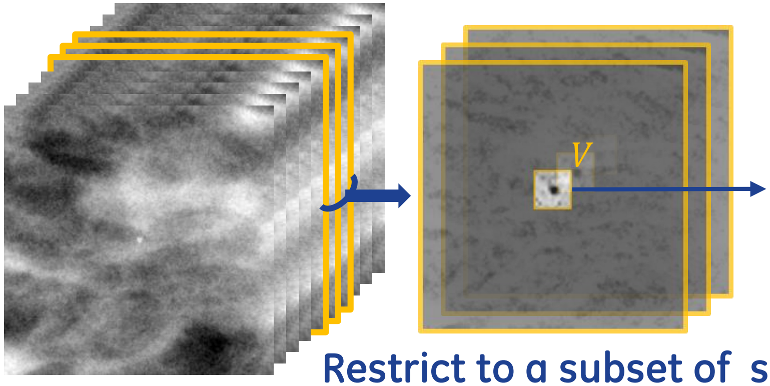

Each selected slice

- Restrict to small neighborhood V

$$\lambda = \min\{\lambda(x) | x \ \in V\}$$

Restrict to a subset of slices

Validation of the new *a contrario* observer

Theoretical proof of false positive control

$$E_{H_0}(\#\{x| \quad \lambda(x) \leq \epsilon\}) < \mathcal{C}(\epsilon)$$

If for all V: $|V| \gg \left(\Phi^{-1}\left(\frac{\epsilon}{t}\right)\right)^2$

→ $C(\epsilon)$: same order of magnitude as ϵ

Experimental validation

200 Scattered fibroglandular dense textures

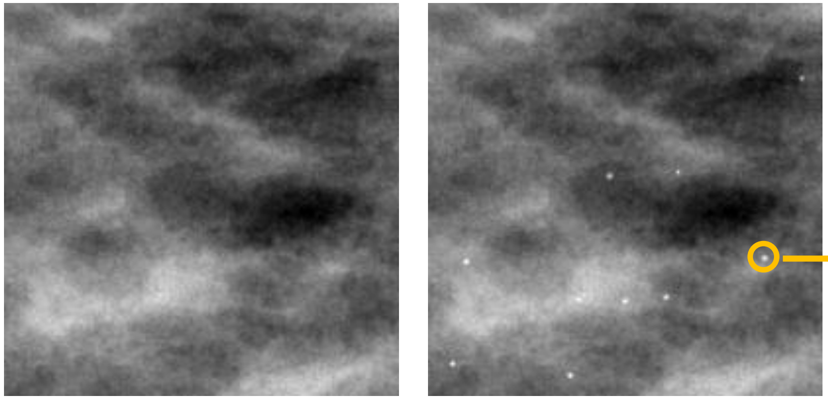

No µcalc

With µcalcs

10 randomly located µcalcs

$$f_i(x) = k \exp\left(\frac{-\|x - c_i\|^2}{0.08\sigma_i^2}\right)$$

σ_i: Uniform ∈ $(200\mu m, 600\mu m)$

Validation of the new *a contrario* observer

Experimental results

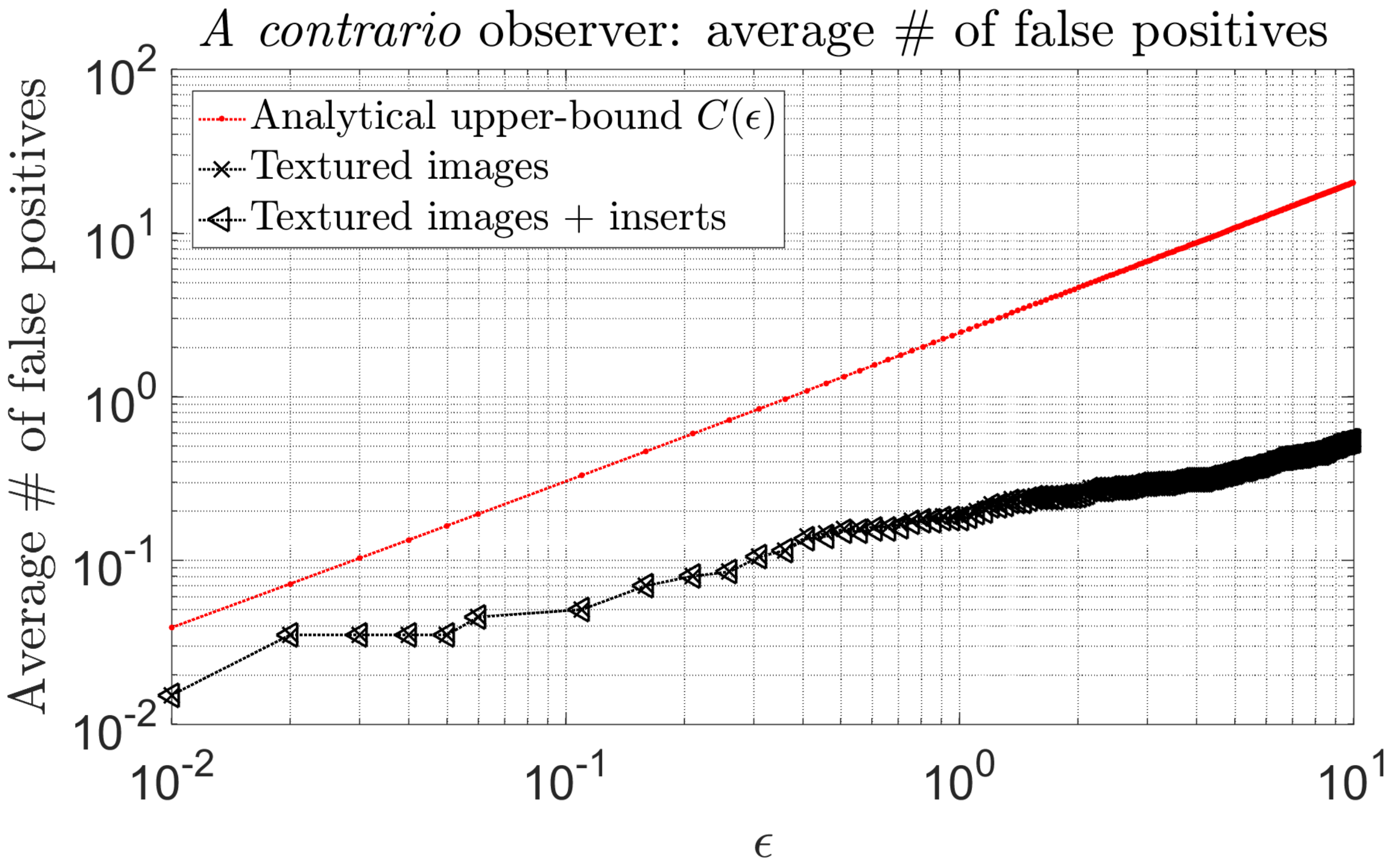

The proposed a contrario observer allows for a global control of false positive detections

Comparison of µcalc detectability in FFDM, DBT & S2D

Application of developed texture model & a contrario observer in a complete VCT study

- Comparison of a contrario observer vs CHO
- Comparison of a contrario observer & CHO vs human observer

Simulated images

2.5 cm x 2.5 cm ROIs, 400µm µCalc highest attenuation

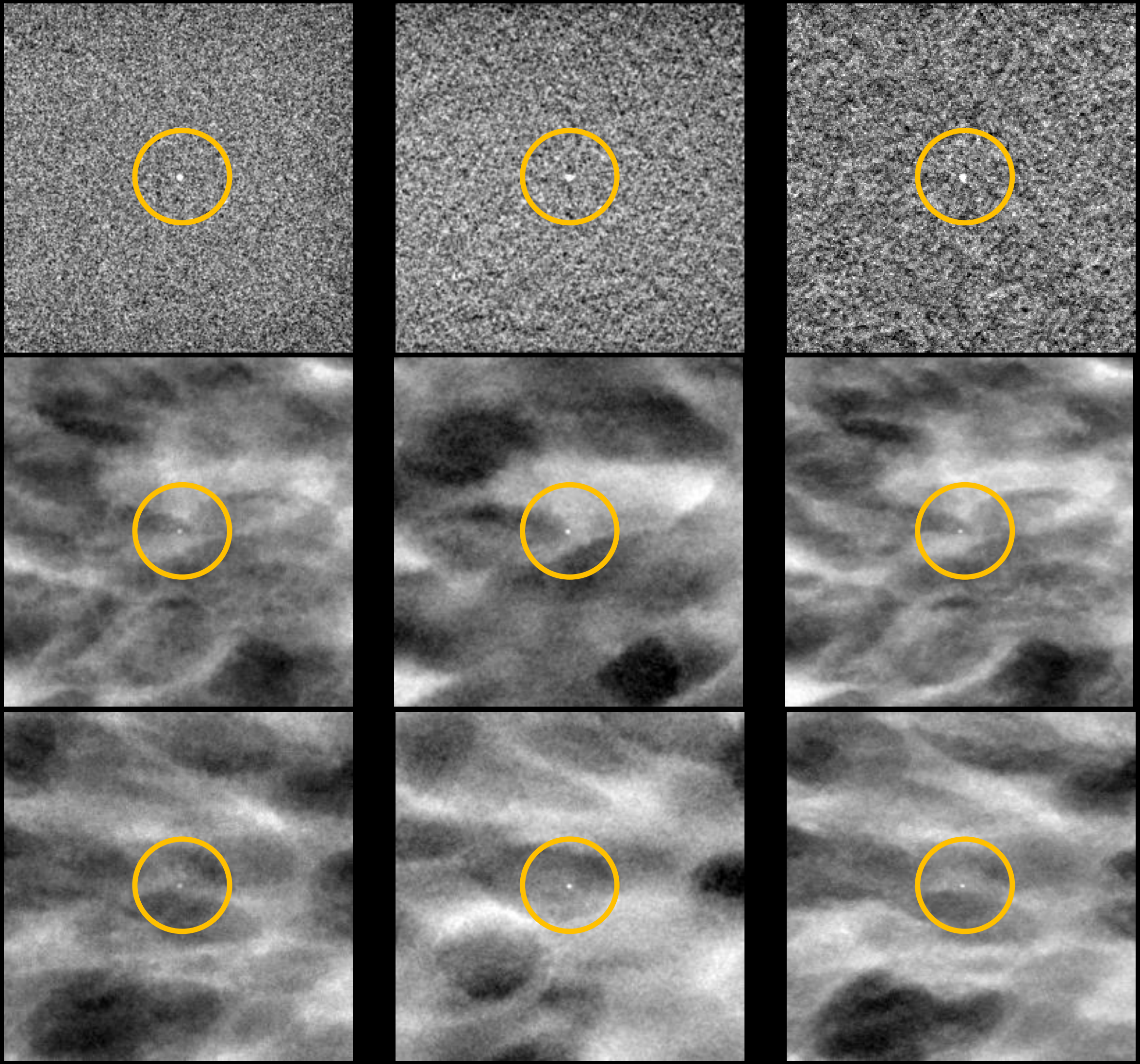

Uniform

Scattered fibroglandular dense

Heterogeneously dense

FFDM

DBT central slice

S2D

Simulated images

2.5 cm x 2.5 cm ROIs, 200µm µCalc highest attenuation

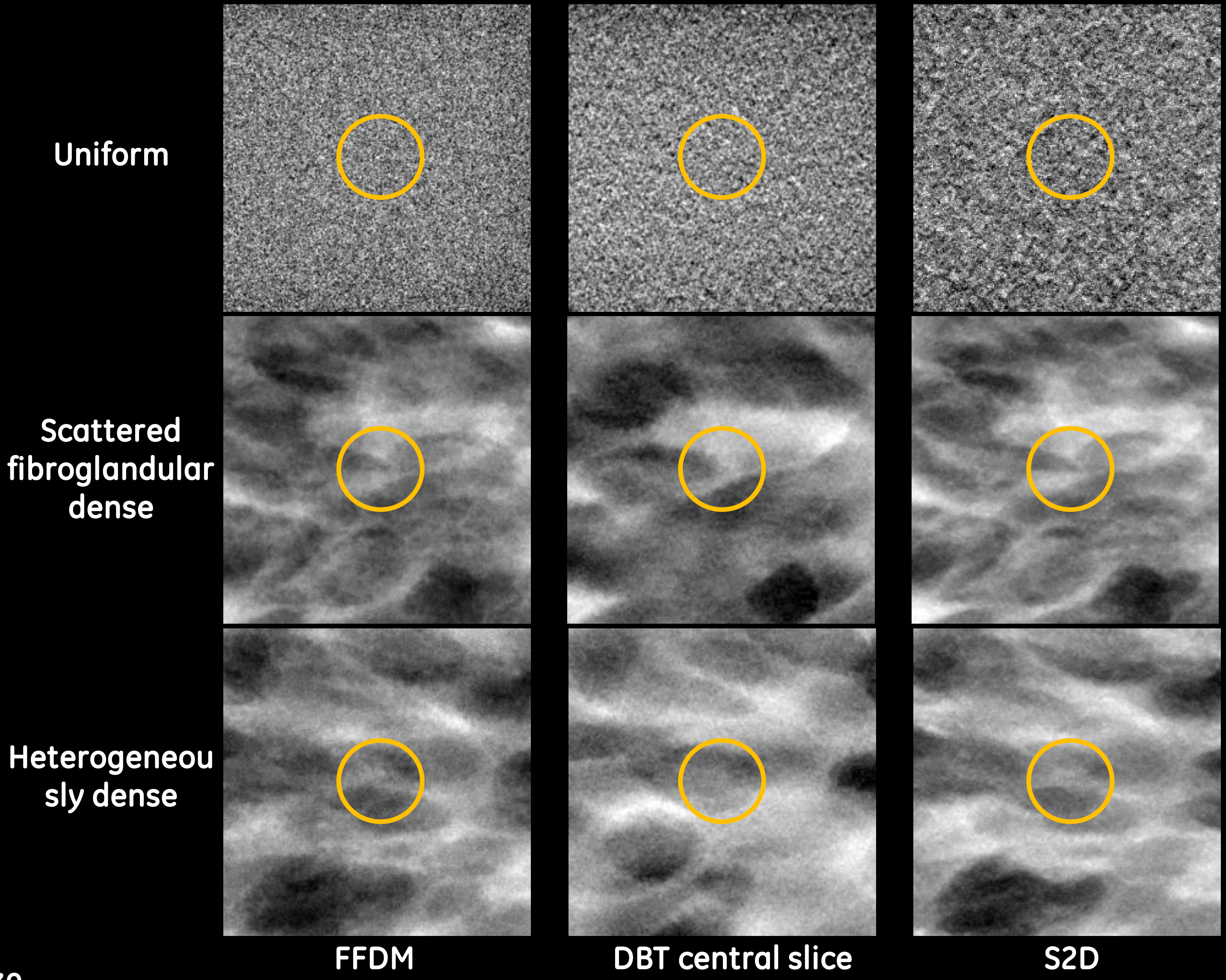

VCT experimental set-up

Task

- Rating scale task
- Signal-known-statistically & location-known-exactly

Observers

- 1 Human observer
- A contrario
- 2D & 3D CHO*

Analysis

- Receiver operator characteristics analysis (ROC)
- Area under the ROC curve (AUC) as figure-of-merit

Image review

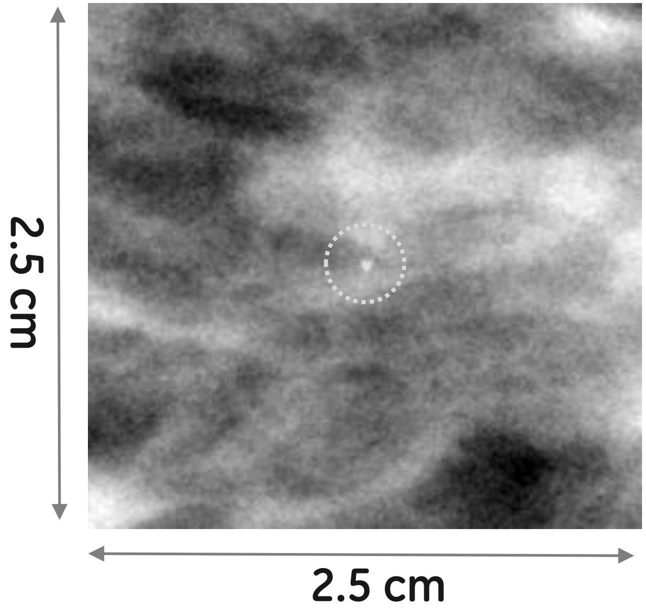

Report confidence for ucalc presence at the center of the image

---

- Platiša, L. *et al*. "Channelized Hotelling observers for the assessment of volumetric imaging data sets". JOSA.

Results

CHO versus *a contrario*

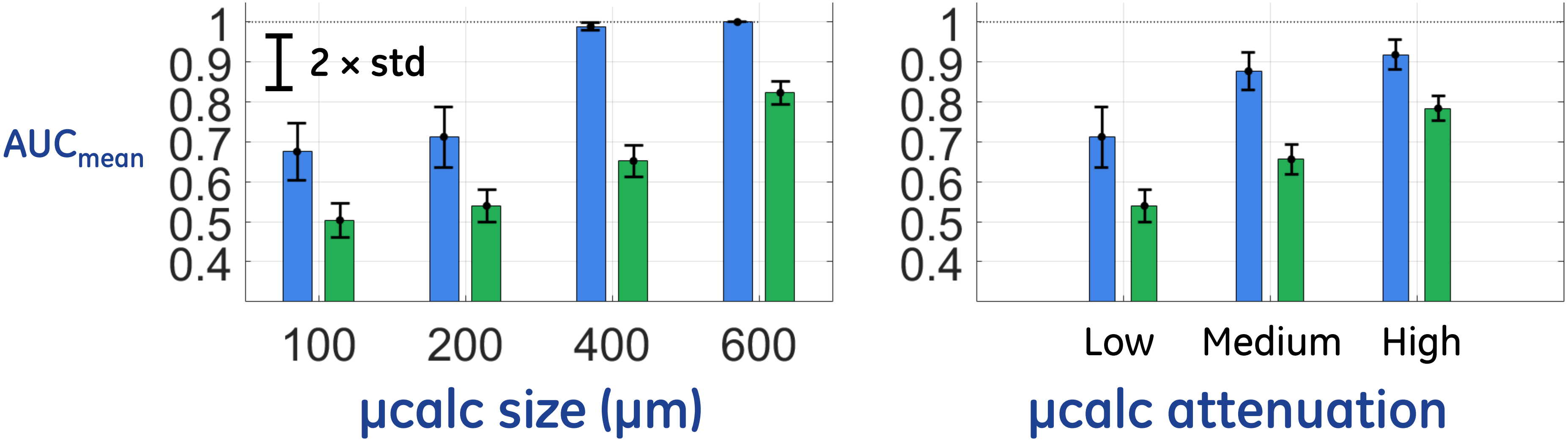

FFDM
heterogeneously dense background

Results

A contrario observer vs CHO

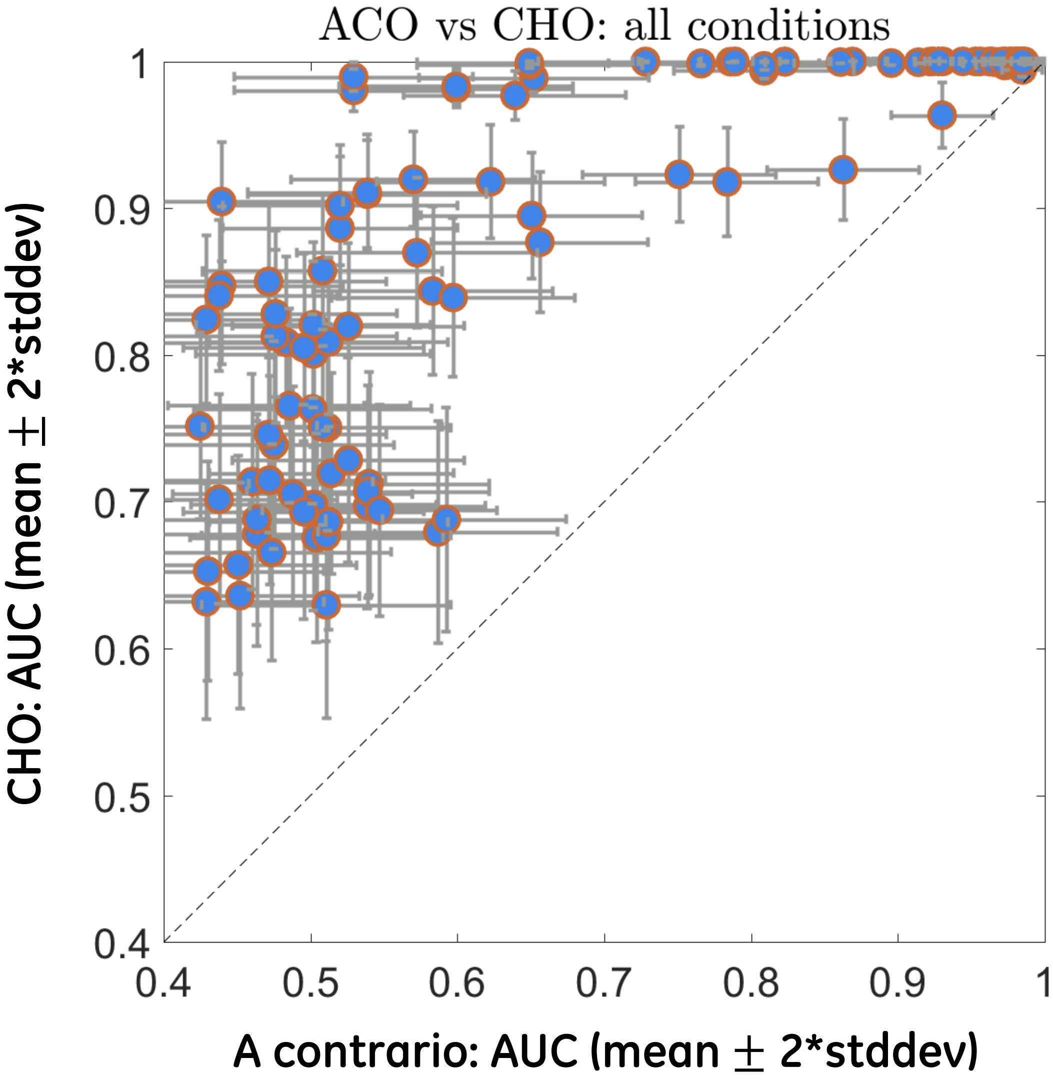

Results

Model observers vs human observer

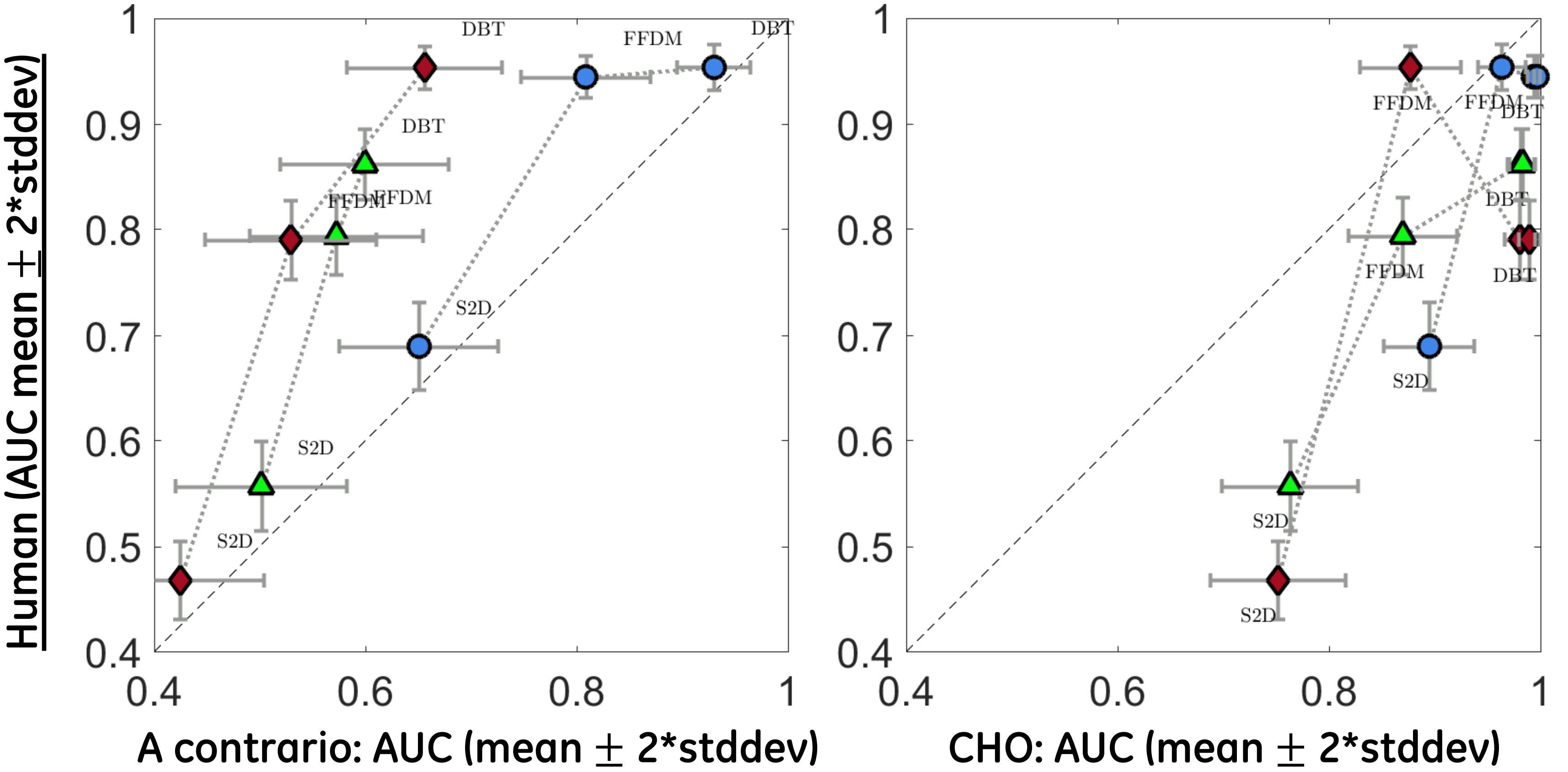

● Uniform background

▲ Scattered fibroglandular dense

◆ Heterogeneously dense

Results

DBT vs FFDM vs S2D (200 µm µcalcs, highest attenuation)

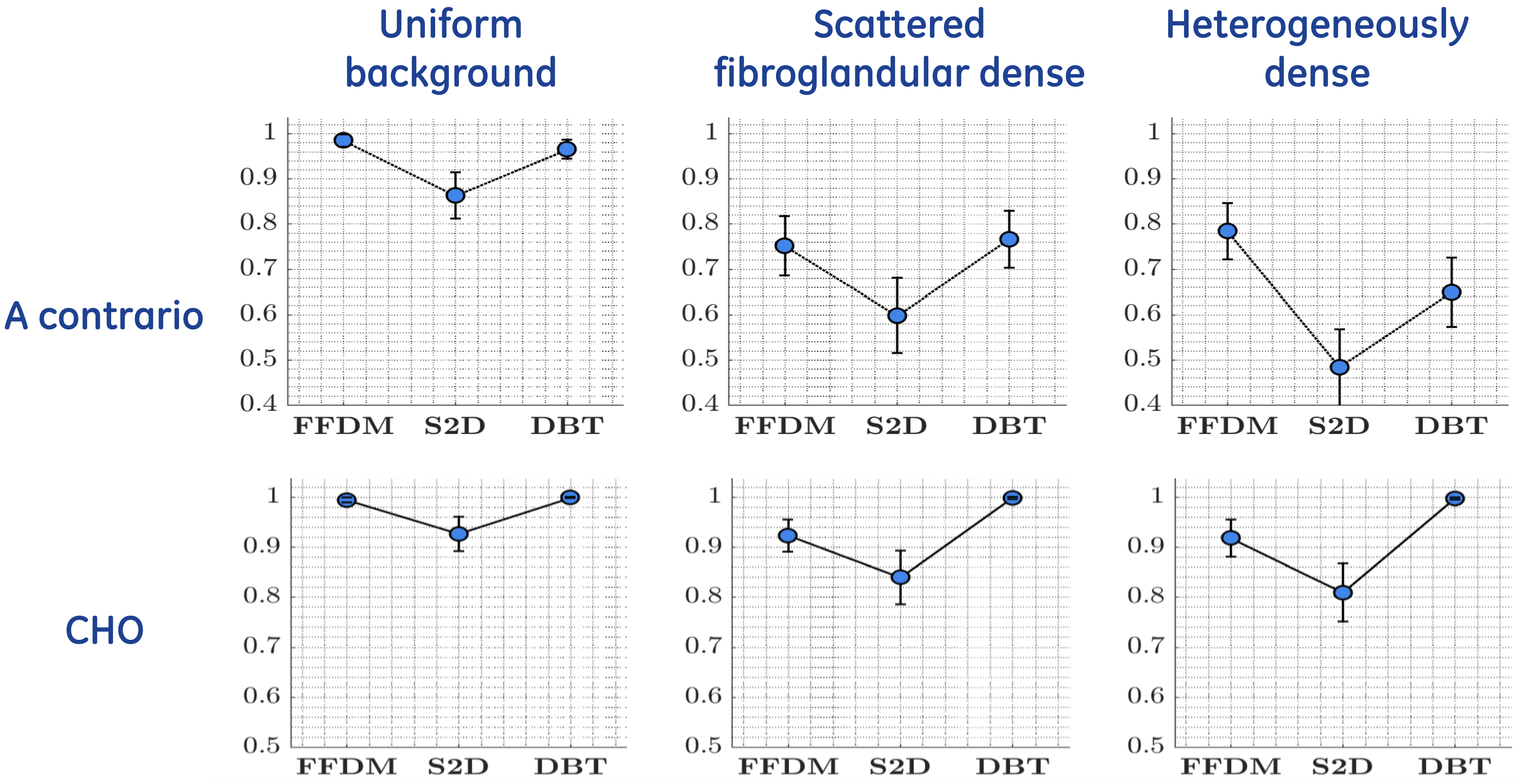

Uniform background

Scattered fibroglandular dense

Heterogeneously dense

A contrario

CHO

Analysis of results

- No clear conclusion on ranking btw modalities: result varies with experimental condition.
- Further set-up refinement needed

- CHO outperforms ACO in all conditions.
- CHO & ACO: tend to be positively correlated to human.

- Demonstration of potential of using developed tools for more elaborated VCT experiments

Main results & contributions

Tools

A new 3D breast texture model

- ✓ Mathematical traceability → stochastic geometric characterization
- ✓ High Realism

A new *a contrario* observer

- ✓ For µcalc detection in 2D breast images & 3D DBT slices
- ✓ An alternative to state-of-the-art models

Methodology

Stochastic geometry

- ✓ Modeling of breast anatomical structures

Inference from reconstruction

- ✓ Medium scale texture model parameters obtained from clinical bCT data
- ✓ Improve texture model morphological variability

Application

Complete VCT experiment assessing µcalc detectability in FFDM, DBT & S2D

- ✓ Demonstrate potential & utility of developed tools

Directions for future research

3D breast texture model

- Statistical validation
- Model other anatomical structures (such as ductal network)

Inference from reconstruction

- Theory study of inference accuracy
- Effect of algorithm initialization
- Correlation btw ellipsoid parameters & center positions
- Unify model to diff. glandular densities
- Statistical & psycho-physical validation

3D *a contrario* observer

- Correlation between DBT slices
- Extension to more complex naive models
- Extension to cluster detection

Thank you !

This study was funded by the French Ministry of Research (ANRT), under CIFRE n° 2013/1052.

CMLA
Centre de Mathématiques et de Leurs Applications

école normale supérieure paris—saclay

anrt
association nationale recherche technologie

GE Healthcare